

Optimization of Space Under Main Deck on Landing Craft Utility (LCU) Ships to Increase Loading Capacity

S. Sugeng, M. Ridwan, S. Sulaiman & S.F. Khristyson
Diponegoro University, Semarang, Indonesia

ABSTRACT: With this optimization, the cargo will increase and the ship's revenue will also be more. The LCU ship that we know so far is a ship whose cargo is always above the main and the space under the main is unused Void Space. The purpose of this study is to determine the optimization value of the use of space under the main deck of the Landing Craft Utility (LCU) ships. method used in this study is a comparison with several previous ship approaches to produce evaluation results from the addition of loading space under the main deck and calculation of stability using computational software approximation. LCU design of under main deck space with a maximum vehicle value can accept a vertical moment of 2750 mm. With a structural strength of 13150 tons. A series of numerical experiments show that the proposed method can effectively produce a satisfactory LCU ship design optimization plan for ship owners.

1 INTRODUCTION

Each shipping operator will always strive for the ship to operate optimally and efficiently in the hope that there will be a better profit margin so that it can support the continuity of the company to be more developed [18, 19]. In this paper the author will present the optimization of space under the main deck for Landing Craft Utility (LCU) ships. With this optimization, the cargo will increase and the ship's revenue will also be more [15, 17]. The LCU ship that we know so far is a ship whose cargo is always above the main and the space under the main is unused Void Space. LCU ships are usually used for crossings between islands with a crossing that is not too far away and contains vehicles or heavy equipment. From the phenomena that exist on passenger ships are usually made to have a high enough loading capacity, see figure 1. This makes passenger ships with optimization of cargo space quite interesting to discuss [1, 21]. Basically, the tank on the ship can be

used to take advantage of the empty space for the placement of vehicles as long as a double bottom construction is made as a replacement [7, 16]. This double bottom construction serves as a buoyancy reserve to provide buoyancy when the ship is operating [5, 11].

Previous research the history of ship design optimization shows that there are several contemporary holistic approaches related to the previous method. The main advantage is that a multi-objective optimization method of ship design problems is solved by considering simultaneously (holistically) all aspects of the ship system design and not as a collection of parts [3, 8]. Based on previous studies, the methodology that is often used begins with the creation of a parametric model that captures the main details and internal compartments of the ship, then with the integration of a numerical tool is developed to determine the performance of each variant of the ship type [13, 20]. This allows an

analysis that can evaluate many functions and design constraints, as well as part of the optimization problem [2, 10]. The differences that have been identified by the previous authors are the lack of a way to capture the uncertainty inherent in the physical environment and a suitable numerical model, an emerging design opportunity that is expected to provide a more pragmatic representation of the solution space to decision makers [4, 8]. Meanwhile several studies show that there is a modern approach to ship design, which is implemented in practice using appropriate software platforms and tools, introducing parametric design into the ship design process, allowing exploration of considerable design space before a decision is made [12, 14]. This approach is often used in the modular ship design process, where the major parts of the ship (hull, engines, fixtures, navigation bridges, etc.) are considered as modules with specific functionality, connectivity, and associated space and weight requirements [6, 9].

The limitation of this research is that the shape used is the development of the LCU ship, and the size of the vehicle used is 16 Light Truck 2.5 Tons on the cargo section of the ship, the calculation includes the stability of the ship with the ability to carry load capacity. The purpose of this study is to determine the optimization value of the use of space under the main deck of the Landing Craft Utility (LCU) ships.

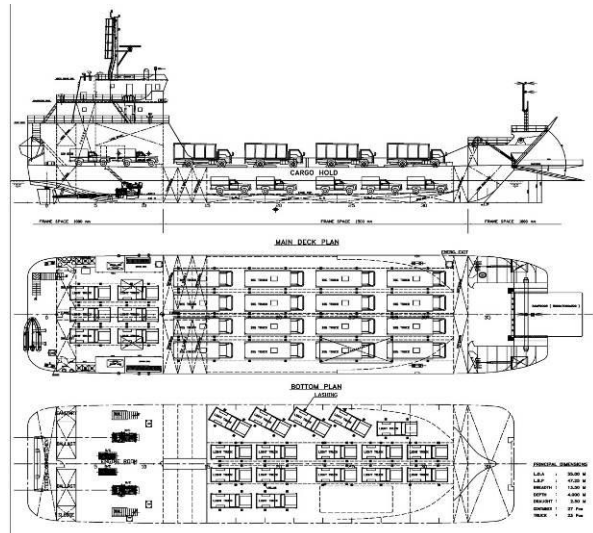


Figure 1. LCU ship after space optimization

Then after calculating the value of the stability of the ship, the data obtained, see table 1.

2 DESCRIPTION

The method used in this study is a comparison with several previous ship approaches to produce evaluation results from the addition of loading space under the main deck. So it is hoped that these additions can provide the best optimization value from this design process, see figure 2.

Table 1. Calculation Stability Criteria LCU ship after space optimization

Item Name	Quant.	Weight tonne	Long. Arm m	Vert. Arm m	Trans. Arm m	FSM tonne.m	FSM Type
Lightship	1	625.3	19.848	4.417	0.000	0.000	
Crews & Effect	1	2.200	7.570	9.710	0.500	0.000	
Provision Store	1	0.500	2.000	9.000	2.500	0.000	
Cargo Hold	1	40.00	28.380	2.200	0.000	0.000	
Cargo on Deck	1	188.7	25.310	5.300	0.000	0.000	
Cargo on M-Deck (under SS)	1	7.500	7.000	4.850	0.000	0.000	
Ballast (aft)p s(fr. 1 s/d 3)	0%	0.0000	2.044	2.730	-2.754	0.000	Maximum
Ballast(aft)sb (fr. 1s/d 3)	50%	11.36	2.088	2.091	2.709	14.538	Maximum
FW. Sanitary (fr.1 s/d 3)	97.9%	6.298	2.077	2.913	-5.711	0.806	Maximum
Sludge (fr. 1 s/d 3)	97.9%	6.298	2.077	2.913	5.711	0.806	Maximum
FO. Settling(ps)(fr.13 s/d 14)	0%	0.000	14.250	2.085	-3.468	0.000	Maximum
FO. Settling(sb)(fr. 13 s/d 14)	20%	5.870	14.250	0.551	2.876	28.750	Maximum
FWT (ps2) (fr.15 s/d 19)	97.9%	17.01	19.508	0.628	-4.261	34.324	Maximum
FWT (sb1) (fr.15 s/d 19)	97.9%	13.15	19.503	0.523	1.168	6.912	Maximum
Ballast (ps) (fr.19 s/d 24)	100%	39.69	26.250	0.588	-2.916	0.000	Maximum
Ballast(sb) (fr.19 s/d 24)	100%	39.69	26.250	0.588	2.916	0.000	Maximum
FOT (ps1) (fr.24 s/d 29)	0%	0.000	33.732	0.535	-1.164	0.000	Maximum
FOT (sb1) (fr.24 s/d 29)	0%	0.000	33.732	0.535	1.164	0.000	Maximum
Ballast (ps)(fr.29 s/d 32)	100%	12.24	39.450	0.640	-1.729	0.000	Maximum
Ballast (sb)(fr.29 s/d 32)	100%	12.24	39.450	0.640	1.729	0.000	Maximum
FPT (fr. 33 s/d)	0%	0.000	45.167	3.097	0.000	0.000	Maximum
FO. Service day Tank (Ps)	97.9%	3.020	4.600	2.932	-1.500	0.490	Maximum
FO. Service day Tank (Sb)	97.9%	3.335	11.350	2.736	3.000	1.258	Maximum
FWT (ps1) (fr.15 s/d 19)	0%	0.000	19.503	0.533	-1.169	0.000	Maximum
FWT (sb2) (fr.15 s/d 19)	0%	0.000	19.507	0.636	4.265	0.000	Maximum
FOT (ps2) (fr.24 s/d 29)	0%	0.000	33.421	0.662	-4.143	0.000	Maximum
FOT (sb2) (fr.24 s/d 29)	0%	0.000	33.421	0.662	4.143	0.000	Maximum
Fixed Ballast	1	38.40	24.650	1.500	-0.047	0.000	UserSpec
Total =		1073	21.590	3.851	-0.003	87.885	FS corr.=
LCG =			21.590	3.851			VCG fluid=
VCG =			21.590	3.851			3.933
TCG =							
FSM =							

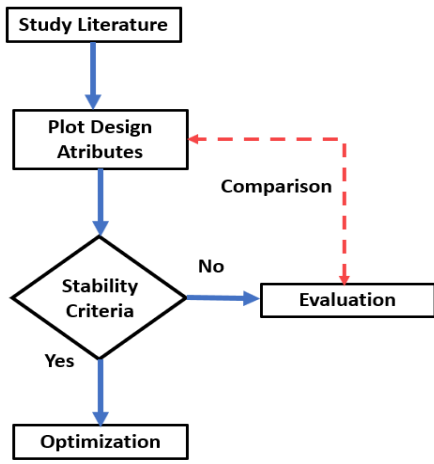


Figure 2. Research Methodology

Calculation of stability using computational software, where the value obtained from the calculated data will later be poured in the form of a graph to make it easier to analyze the results of the study. Results of the evaluation of the addition of space under the main deck become a separate consideration for ship designers to provide a good loading and unloading system as well. system in question is an elevator, see Figure 3.

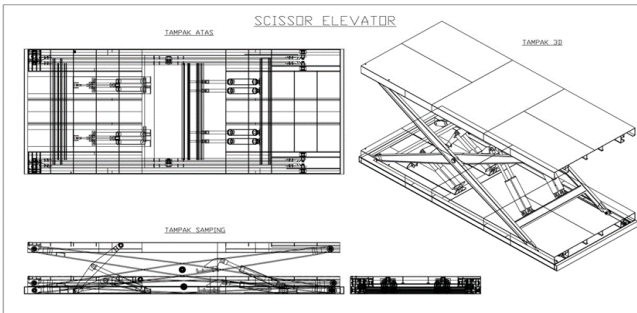


Figure 3. Elevator Cassis

The elevation system mounted on the ship is a lift system design that makes it easy for vehicles to access up and down. This system does not require a lot of space for operational processes, however it requires hydraulic power and limits on the weight of trucks that can be accessed for the up and down process. The standard used in this stability calculation is in accordance with the IMO standard, see figure 4.

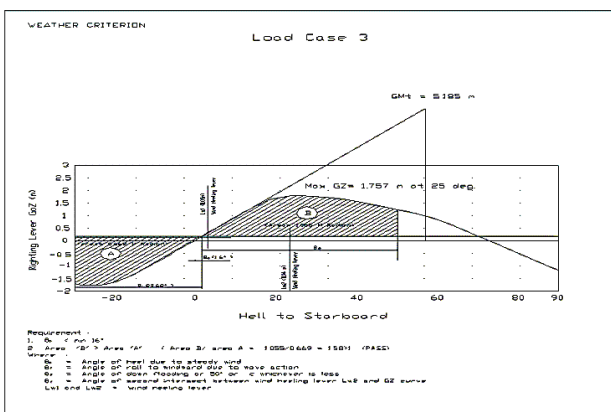


Figure 4. Load Case Criteria

3 RESULTS OF THE MEASUREMENTS

From the design attributes, the design of this additional loading space is categorized into several models which are illustrated by Figure 5.

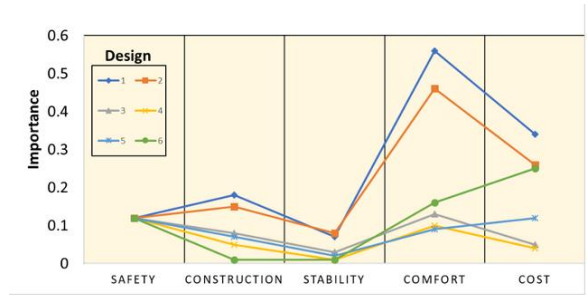


Figure 5. Design by Importance

Some of these aspects indicate the need to review several considerations in determining the design.

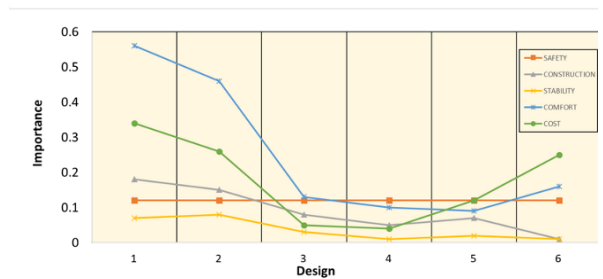


Figure 6. Importance by Design

From this comparison, it can be seen that designs 1 and 2 have the closest parameters, where in terms of the comfort level, the value is very high, while the cost of each has a value that is relatively almost the same. From designs 1 and 2, stability analysis was then carried out and then obtained the results of the stability criteria as set out in Figure 7.

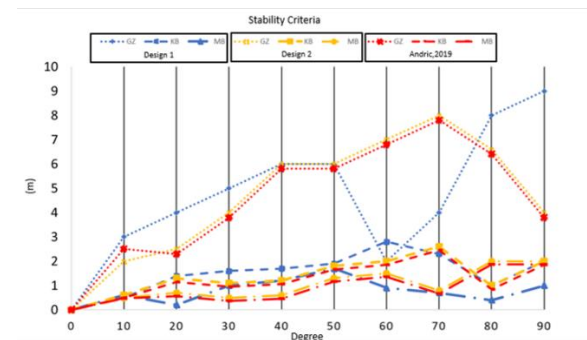


Figure 7. Stability Criteria

Results show the value of GZ at an angle of 70 degrees in design 2 is better than the previous researchers and design 1. From a fairly critical angle, the length of the moment arm returns to its original position up to 7.6 m. In balance with the distance from Keel to Metacenter and Keel to Buoyancy which shows a good trend as well. Results of the comparison of VCG with IMO show conditions that meet the standard requirements, see table 2. So that this second design can be used as a reference in optimizing the space under the main deck to increase the capacity of the ship's truck loading space.

Table 2. Result VCG comparison with IMO standard

Code	Criteria	Value	Units	Actual	Remark
A.749(18) Ch3 – Design criteria applicable to all ships	3.1.2.1: Area 0 to 30	0.055	m.rad	0.165	Pass
	3.1.2.1: Area 0 to 40	0.090	m.rad	0.899	Pass
	3.1.2.1: Area 30 to 40	0.030	m.rad	0.287	Pass
	3.1.2.2: Max GZ at 30 or greater	0.200	m	1.757	Pass
	3.1.2.3: Angle of maximum GZ	25.0	deg	25.0	Pass
	3.1.2.4: Initial GMt	0.150	m	5.185	Pass
A.749(18) Ch3 – Design criteria applicable to all ships	3.2.2: Severe wind and rolling				Pass
	Wind arm: $a = P A (h - H) / (g \text{ disp.}) \cos^n(\phi)$	0.99			
	constant: a =	504.00	Pa		
	wind pressure: P =	6.344	m		
	area centroid height (from zero point): h =	278.640	m ²		
	total area: A =	1.133	m		
	H = mean draught / 2	0			
	cosine power: n =	1.5			
	gust ratio				
	Area2 integrated to the lesser of roll back angle from equilibrium (with steady heel arm)	1.0 (-0.3)	deg	-0.3	
	Area 1 upper integration range, to the lesser of:				
	angle of max. GZ	25.0	deg	25.0	
	angle of max. GZ above gust heel arm	25.0	deg		
	Angle for GZ(max) in GZ ratio, the lesser of:				
	spec. heel angle	45.0	deg	45.0	
	Select required angle for angle of steady heel ratio:				
	Deck Edge Immersion Angle				Pass
	Angle of steady heel shall not be greater than (\leq)	16.0	deg	0.7	Pass
	Area1 / Area2 shall not be less than (\geq)	100.000	%	27427.2	Pass
	Area 1 shall not be less than (\geq)	0.000	m.rad	0.414	Pass
	Intermediate values				
	Heel arm amplitude		m	0.069	
	Equilibrium angle with steady heel arm		deg	0.7	
Equilibrium angle with gust heel arm		deg	1.1		
Area1 (under GZ), from 1.1 to 25.0 deg.		m.rad	0.457		
Area1 (under HA), from 1.1 to 25.0 deg.		m.rad	0.043		
Area1, from 1.1 to 25.0 deg.		m.rad	0.414		
Area2 (under GZ), from -0.3 to 1.1 deg.		m.rad	0.001		
Area2 (under HA), from -0.3 to 1.1 deg.		m.rad	0.002		
Area2, from -0.3 to 1.1 deg.		m.rad	0.002		
Area B / Area A = 1.055/0.669		1.000	1.580	Pass	

4 DISCUSSION OF RESULTS

From the comparison results of several models and previous studies, it is known that the LCU design value still enters the IMO criteria. This can be seen from the VCG value and the mass structure which is quite ideal for the number of vehicles accommodated, see figure 8

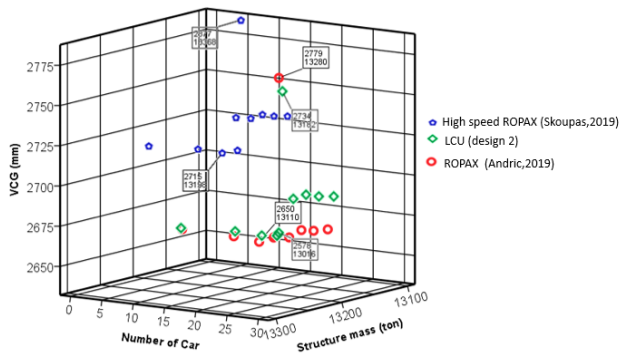


Figure 8. VCG Comparison and Structure mass

LCU design of under main deck space with a maximum vehicle value can accept a vertical moment of 2750 mm. With a structural strength of 13150 tons, it still shows a fairly good capacity from the design attribute, which has a significant value. This is in line

with previous research which showed the influence of the increasing number of vehicle capacities that can be loaded, the more vertical gravity is formed.

5 FINAL CONCLUSIONS

The second design is designed to get a car layout with the maximum level of comfort and total convenience. In order to reduce the problems related to the carrying capacity of the vehicle, a ship rolling-stability heuristic approach based on VCG feedback (positive and negative) was taken into account. Based on the guidance mechanism, the results of the structure mass calculation describe the guidance provided by the existing vehicle layout to the room below the main deck, while based on the elevator system mechanism, it is a solution to access vehicle arrivals to the vehicle layout. A series of numerical experiments show that the proposed method can effectively produce a satisfactory LCU ship design optimization plan for ship owners.

REFERENCES

- Andersson, J. et al.: Review and comparison of methods to model ship hull roughness. Applied Ocean Research.

- 99, 102119 (2020). <https://doi.org/10.1016/j.apor.2020.102119>.
2. Andric, J. et al.: Influence of different topological variants on optimized structural scantlings of passenger ship. *Marine Structures*. 78, 102981 (2021). <https://doi.org/10.1016/j.marstruc.2021.102981>.
 3. Andric, J. et al.: Multi-level Pareto supported design methodology- application to RO-PAX structural design. *Marine Structures*. 67, 102638 (2019). <https://doi.org/10.1016/j.marstruc.2019.102638>.
 4. Bulian, G. et al.: Complementing SOLAS damage ship stability framework with a probabilistic description for the extent of collision damage below the waterline. *Ocean Engineering*. 186, 106073 (2019). <https://doi.org/10.1016/j.oceaneng.2019.05.055>.
 5. Cepowski, T.: The prediction of ship added resistance at the preliminary design stage by the use of an artificial neural network. *Ocean Engineering*. 195, 106657 (2020). <https://doi.org/10.1016/j.oceaneng.2019.106657>.
 6. Dogrul, A. et al.: Scale effect on ship resistance components and form factor. *Ocean Engineering*. 209, 107428 (2020). <https://doi.org/10.1016/j.oceaneng.2020.107428>.
 7. Francescutto, A.: Intact stability criteria of ships – Past, present and future. *Ocean Engineering*. 120, 312–317 (2016). <https://doi.org/10.1016/j.oceaneng.2016.02.030>.
 8. Fu, T. et al.: Simulating the dynamic behavior and energy consumption characteristics of frozen sandy soil under impact loading. *Cold Regions Science and Technology*. 166, 102821 (2019). <https://doi.org/10.1016/j.coldregions.2019.102821>.
 9. Jafaryeganeh, H. et al.: Application of multi-criteria decision making methods for selection of ship internal layout design from a Pareto optimal set. *Ocean Engineering*. 202, 107151 (2020). <https://doi.org/10.1016/j.oceaneng.2020.107151>.
 10. Kaidi, S. et al.: Numerical modelling of the muddy layer effect on Ship's resistance and squat. *Ocean Engineering*. 199, 106939 (2020). <https://doi.org/10.1016/j.oceaneng.2020.106939>.
 11. Peng, H. et al.: Wave pattern and resistance prediction for ships of full form. *Ocean Engineering*. 87, 162–173 (2014). <https://doi.org/10.1016/j.oceaneng.2014.06.004>.
 12. Priftis, A. et al.: Multi-objective robust early stage ship design optimisation under uncertainty utilising surrogate models. *Ocean Engineering*. 197, 106850 (2020). <https://doi.org/10.1016/j.oceaneng.2019.106850>.
 13. Skoupas, S. et al.: Parametric design and optimisation of high-speed Ro-Ro Passenger ships. *Ocean Engineering*. 189, 106346 (2019). <https://doi.org/10.1016/j.oceaneng.2019.106346>.
 14. Song, S. et al.: Validation of the CFD approach for modelling roughness effect on ship resistance. *Ocean Engineering*. 200, 107029 (2020). <https://doi.org/10.1016/j.oceaneng.2020.107029>.
 15. Tan, X. et al.: Preliminary design of a tanker ship in the context of collision-induced environmental-risk-based ship design. *Ocean Engineering*. 181, 185–197 (2019). <https://doi.org/10.1016/j.oceaneng.2019.04.003>.
 16. Terziev, M. et al.: A posteriori error and uncertainty estimation in computational ship hydrodynamics. *Ocean Engineering*. 208, 107434 (2020). <https://doi.org/10.1016/j.oceaneng.2020.107434>.
 17. Tillig, F., Ringsberg, J.W.: Design, operation and analysis of wind-assisted cargo ships. *Ocean Engineering*. 211, 107603 (2020). <https://doi.org/10.1016/j.oceaneng.2020.107603>.
 18. Weintrit, A., Neumann, T.: Advances in marine navigation and safety of sea transportation. Introduction. *Advances in Marine Navigation and Safety of Sea Transportation - 13th International Conference on Marine Navigation and Safety of Sea Transportation, TransNav 2019*. 1 (2019).
 19. Weintrit, A., Neumann, T.: Safety of marine transport introduction. In: *Safety of Marine Transport: Marine Navigation and Safety of Sea Transportation*. pp. 1–4 (2015).
 20. Yuan, Y. et al.: A design and experimental investigation of a large-scale solar energy/diesel generator powered hybrid ship. *Energy*. 165, 965–978 (2018). <https://doi.org/10.1016/j.energy.2018.09.085>.
 21. Zhang, W. et al.: An integrated ship segmentation method based on discriminator and extractor. *Image and Vision Computing*. 93, 103824 (2020). <https://doi.org/10.1016/j.imavis.2019.11.002>.